Orientational Control of Colloidal 2D-Layered Transition Metal Dichalcogenide Nanodiscs *via* Unusual Electrokinetic Response

Daniel Rossi,[†] Jae Hyo Han,[‡] Wonil Jung,[‡] Jinwoo Cheon,[‡] and Dong Hee Son*[,†]

[†]Department of Chemistry, Texas A&M University, College Station, Texas 77843, United States and [‡]Department of Chemistry, Yonsei University, Seoul, South Korea

ABSTRACT We report an unusual response of colloidal layered transition metal dichalcogenide (TMDC) nanodiscs to the electric field, where the orientational order is created transiently only during the time-varying period of the electric field while no orientational order is created by the DC field. This result is in stark contrast to the typical electrokinetic response of various other colloidal nanoparticles, where the permanent dipole or (and) anisotropic-induced dipole creates a sustaining orientational order under the DC field. This indicates the lack of a sizable permanent dipole or (and) anisotropic-induced dipole in colloidal TMDC nanodiscs, despite their highly anisotropic lattice structure. While the orientational order is created only transiently by the time-varying field, a near-steady-state orientational order can be obtained by using an AC electric field. We demonstrate the utility of this method for the controlled orientation of colloidal nanoparticles that cannot be controlled *via* the usual interaction of the electric field with the nanoparticle dipole.

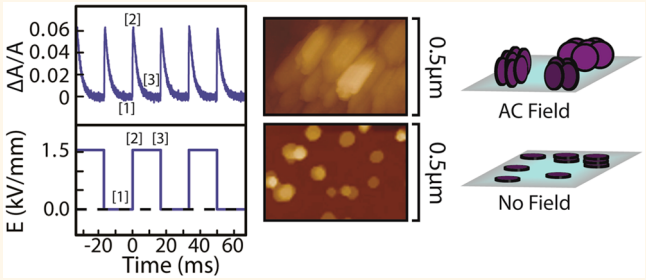

KEYWORDS: two-dimensional nanostructure · transition metal dichalcogenide · electric-field-induced orientation

Single- and few-layer transition metal dichalcogenide (TMDC) materials are attracting much attention due to their unique optical, electronic, and transport properties arising from the two-dimensional confinement within the layer combined with a variable interlayer interaction.[1,2] The tunable optical and electronic properties *via* control of the number of layers makes the single- and few-layer TMDCs particularly attractive for various optoelectronic applications.[3−7] So far, the majority of atomically thin TMDC nanostructures have been created *via* either chemical vapor deposition (CVD) or exfoliation from the bulk. While these methods are capable of achieving fine control over the material thickness and have enabled the discovery of new properties of atomically thin TMDCs, they also have limitations in scaling up the synthesis and controlling the lateral dimension.[8,9]

More recently, solution-phase synthetic methods capable of producing colloidal TMDC nanodiscs dispersed in liquid media with simultaneous control of both the thickness and lateral dimension have been developed.[10] These colloidal TMDC nanoparticles offer the unique opportunity to explore the multidimensional dependence of the TMDC properties, which has been difficult to address with sheets and flakes from CVD and exfoliation methods. For example, one can utilize a variety of methods for manipulating the movement and assembling behavior of colloidal particles to create structures with higher order and controlled orientation. For TMDC nanodiscs with strongly anisotropic optical and transport properties, the capability to control their orientation will be particularly useful to exploit their anisotropic material properties.[11,12]

One strategy to achieve orientational control is to apply an external electric or magnetic field that creates an anisotropic potential energy landscape, allowing particle alignment through the interaction between the particles' magnetic/electric dipole and the applied field.[13,14] For instance, the alignment of semiconducting and metallic rods to a preferential direction has been

* Address correspondence to dhson@chem.tamu.edu.

Received for review March 16, 2015 and accepted July 30, 2015.

Published online July 30, 2015
10.1021/acsnano.5b01631

achieved *via* interaction of the electric field with the permanent dipole or anisotropic-induced dipole.[14−17] For the group of layered TMDC materials possessing inversion symmetry, one would generally anticipate a relatively weak permanent dipole, which is less desirable for electric-field-induced control of the orientation. On the other hand, the anisotropic 2D crystal structure may produce a large anisotropy of the induced dipole, which can potentially be utilized to align the TMDC nanodiscs even in the absence of a sufficiently large permanent dipole. Contrary to our expectation, we observed the complete absence of orientational order in several different colloidal TMDC nanodiscs under ~kV/mm DC electric fields, which can readily align one-dimensional CdS nanorods with permanent dipoles. This suggests that neither the permanent dipole nor the anisotropic-induced dipole of these nanodiscs is sufficiently large to create an orientational order in response to the applied DC electric field. However, the unexpected transient alignment of the colloidal TMDC nanodiscs created by the time variation of the electric field, such as at the step edges of the square wave field, was observed, as shown in Figure 1a−c. This behavior is in distinct contrast to the typical response of the anisotropic colloidal nanoparticles to the electric field, such as in CdS nanorods shown in Figure 1d−f, where the sustaining orientational order is created during the field-on period and randomizes *via* rotational relaxation during the field-off period.

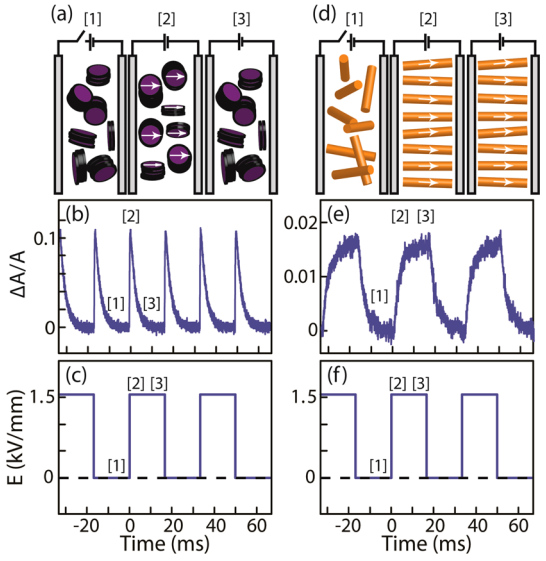

Figure 1. (a,d) Illustration of the random and oriented states of the colloidal nanoparticles under the square wave electric field for (a) TiS_2 nanodiscs and (d) CdS nanorods. [1], [2], and [3] indicate low, step edge, and high state of the electric field, respectively. (b,e) Electro-optic response of (b) TiS_2 nanodiscs in cyclohexane and (e) CdS nanorods in tetradecane to the square wave electric field shown in (c) and (f), respectively. $\Delta A/A$ is the fractional change in the absorbance measured with linearly polarized light representing the presence of the orientational order.

In this study, we investigated the unusual transient electrokinetic response of the colloidal TMDC nanodiscs using linear dichroism to probe the orientational order under various time-varying electric fields. We also showed that near-steady-state orientational order can be obtained from high-frequency AC fields, despite the lack of usual interactions between the nanoparticle dipole and the DC electric field giving rise to the typical electric-field-induced ordering of colloidal nanoparticles. The capability to create a sustaining orientational order, even in the absence of a sufficiently strong permanent dipole or anisotropic-induced dipole, opens a new alternative route to control the orientation of the colloidal TMDC nanodiscs. Utilizing the near-steady-state orientational order created under the AC field, we demonstrate the capability to control the surface orientation of the TMDC nanodiscs deposited on a solid substrate and measured the orientation-dependent optical spectra of the surface-deposited samples. The observation made in this study adds a valuable strategy to control the orientation of the colloidal TMDC nanocrystals, allowing the exploration of their highly anisotropic properties.

RESULTS AND DISCUSSION

In this study, the electric-field-induced orientation of three different colloidal layered TMDC nanodisc samples (TiS_2, WSe_2, and ZrS_2) was investigated by measuring the electro-optic response probing the linear dichroism of the interband transition.[18,19] Since the interband transition in various TMDC materials is considered to be strongly in-plane polarized, linear dichroism can readily detect changes in orientational order. Figure 2 shows two different configurations of the parallel electrodes, which were used to apply a spatially homogeneous electric field perpendicular (E_x) and parallel (E_z) to the propagation direction (k) of the light. The polarization angle (θ_p) of light, controlled by a polarizer, was defined with respect to the direction of the E_x field. The details of the measurement and sample preparation are described in the Methods section. Since the electro-optic responses from all three samples are similar, we focus our discussion on TiS_2 nanodiscs, which have a more uniform size distribution

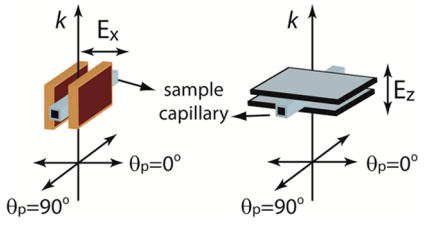

Figure 2. Electrode configurations for the electric field perpendicular (E_x) and parallel (E_z) to the light propagation direction (k). The glass sample capillary was sandwiched between the two electrodes. The polarization of light (θ_p) is defined with respect to the direction of the E_x field.

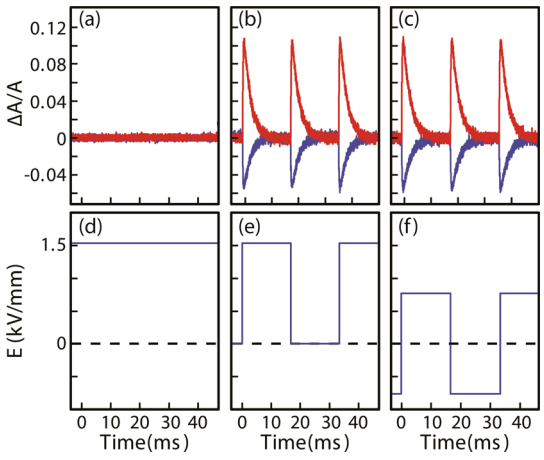

Figure 3. $\Delta A/A$ of TiS_2 nanodisc under (a) DC and (b,c) square wave E_x electric field. Polarization angle of light is $\theta_p = 0°$ (red) and $\theta_p = 90°$ (blue). (d−f) Time variation of the DC and square wave electric field corresponding to panels (a−c), respectively.

and stronger absorption in the visible spectral range for ease of measurement. The electro-optic response from the other two nanodisc samples can be found in Supporting Information.

Figure 3a−c shows the fractional changes in the absorption ($\Delta A/A$) from TiS_2 nanodiscs dispersed in cyclohexane under the DC and square wave E_x electric fields relative to the no-field condition. The red and blue curves were obtained with $\theta_p = 0$ and 90° polarization, respectively. The electric field time profiles corresponding to the data are shown in Figure 3d−f. Under the DC electric field (Figure 3a), there is no steady-state change in the absorption spectra for either polarization, indicating the absence of any orientational order. In contrast, a strong linear dichroism is observed at both the rising and the falling edge of the applied square wave field, as shown in Figure 3b,c. Interestingly, the dichroism at the field edges decays on a few millisecond time scale even when the field is sustained. Furthermore, the comparisons shown in Figure 3b,c indicate that the magnitude of the dichroism is independent of the DC field offset and dependent only on the step height (ΔE) at the field edges, as discussed in detail below. While the typical electric-field-induced dichroism in colloidal particles reflects the orientational order, the origin of the transient dichroism observed in TiS_2 nanodiscs should be more carefully examined considering its unusual behavior. When the dichroism reflects the orientational order, it should exhibit a well-defined dependence on the relative direction of the light polarization with respect to the direction of preferred particle orientation.[20] This is because the absorption (A) of the spheroids depends on the angle (γ) between the light polarization and the major axis of the spheroid as $A = A_{\parallel} \cos^2 \gamma + A_{\perp} \sin^2 \gamma$, where $A_{\parallel}$ and $A_{\perp}$ are the absorption parallel and perpendicular to the major axis, respectively.[21]

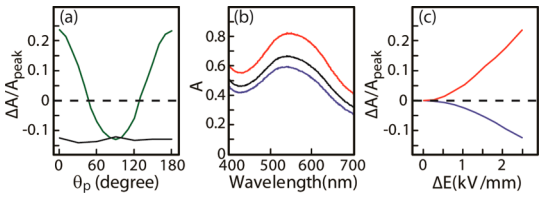

Figure 4. (a) Polarization angle (θ_p) dependence of $\Delta A/A_{peak}$ under the square wave E_x (green) and E_z (black) electric field. $\Delta A/A_{peak}$ is the peak value of the fractional change in the absorbance from the square wave electric field. (b) Absorption spectra of TiS_2 nanodiscs under square wave E_x field with $\Delta E = 2.5$ kV/mm for $\theta_p = 0°$ (red) and $\theta_p = 90°$ (blue) polarization. Black curve is the isotropic absorption spectrum taken without electric field. (c) ΔE dependence of $\Delta A/A_{peak}$ under the square wave E_x field for $\theta_p = 0°$ (red) and $\theta_p = 90°$ (blue) polarization.

In order to confirm that the observed dichroism in TiS_2 nanodiscs reflects the orientational order, $\Delta A/A$ was measured as a function of the polarization angle under both E_x and E_z electric field. Figure 4a shows the peak value of the fractional change in the absorbance ($\Delta A/A_{peak}$) from TiS_2 nanodiscs as a function of the polarization angle (θ_p) under square wave E_x (green) and E_z (black) electric fields. For both electric fields, the step height at the field edge (ΔE) was ~2.5 kV/mm. $\Delta A/A_{peak}$ under the E_x electric field can be fit to $a \cdot \cos^2 \theta_p + b$, and the ratio of $\Delta A/A_{peak}$ at $\theta_p = 0$ and 90° is −(2:1). $\Delta A/A_{peak}$ is zero near the magic angle ($\theta_p = 54.7°$), where the absorption is equivalent to that of the randomly oriented nanodiscs. Under the E_z electric field, $\Delta A/A_{peak}$ is independent of the polarization angle and its magnitude is close to $\Delta A/A_{peak}$ at $\theta_p = 90°$ under the E_x electric field. The $\cos^2 \theta_p$ dependence of the $\Delta A/A_{peak}$ under the E_x electric field is indicative of optically anisotropic particles with orientational order. This indicates that the observed dichroism of the TiS_2 nanodiscs originates from the electric-field-induced alignment, despite its unusual transient nature and independence on the fields' DC amplitude. Since the absorption is strongly in-plane polarized, the positive and negative signs of $\Delta A/A_{peak}$ for $\theta_p = 0$ and 90° polarization under the E_x field in Figure 4a indicate that the TiS_2 nanodiscs align with the in-plane axis parallel to the applied electric field, as illustrated in Figure 1a.[6,19,22] Taking advantage of the transient orientational order created at the edges of the square wave field, we were also able to obtain the anisotropic absorption spectra in the visible spectral range using a pulsed light source synchronized to the edges of the square wave electric field. Figure 4b compares the anisotropic absorption spectra taken at $\theta_p = 0°$ (red) and 90° (blue) under the E_x square wave field with $\Delta E = \sim 2.5$ kV/mm. The isotropic absorption spectrum (black) taken in the absence of the field is also shown. The line shapes of the two spectra at $\theta_p = 0$ and 90° are similar, which is consistent with the dominant contribution from the in-plane transitions to the overall absorption of TiS_2 nanodiscs. On the other

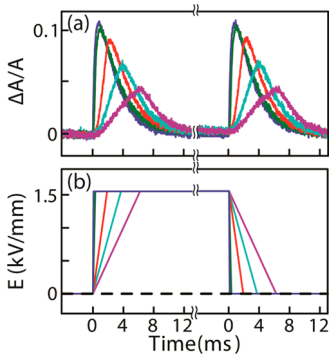

Figure 5. (a) $\Delta A/A$ of TiS_2 nanodiscs measured with $\theta_p = 0°$ polarization under trapezoidal E_x fields with varying slopes at the edges. (b) Time profile of the applied E_x electric field.

hand, the spectrum for $\theta_p = 90°$ is slightly blue-shifted with respect to $\theta_p = 0°$, as will be further discussed later.

As shown in Figure 3, the magnitude of the dichroism from the transient orientational order depends only on the step height (ΔE) at the edges of the square wave field, not on the absolute amplitude of the DC field. To examine the correlation between ΔE and the magnitude of the transient orientational order, $\Delta A/A_{peak}$ was measured as a function of ΔE under the E_x square wave field for $\theta_p = 0°$ (red) and 90° (blue) light polarizations (Figure 4c). The magnitude of $|\Delta A/A_{peak}|$ increases with increasing ΔE, and the dependence is superlinear at relatively small values of ΔE for both light polarizations. Interestingly, the dependence of $\Delta A/A_{peak}$ on ΔE in TiS_2 nanodiscs is similar to typical E dependence of the electro-optic response from colloidal particles with permanent dipole or anisotropic-induced dipoles.[16,20,23] This observation indicates that the change in field amplitude (ΔE) is the key parameter that determines the magnitude of the electric-field-induced orientational order in colloidal TiS_2 nanodiscs. To examine the effect of varying the field sweep rate (dE/dt) for a given ΔE on the orientational order, $\Delta A/A$ was measured under trapezoidal E_x electric fields of varying slopes at the rising and falling edges for $\theta_p = 0°$ polarization, as shown in Figure 5a. For each trapezoidal field shown in Figure 5b, $\Delta A/A$ increases continuously during the entire period of the time-varying electric field at both the rising and falling edges of the field. On the other hand, with decreasing field sweep rate (dE/dt) at the edges of the trapezoidal field, the peak of $\Delta A/A$ also decreases. This reflects the strong competition between the rise and decay of the orientational order, where the dynamics of the rise of the orientational order varies with dE/dt, while that of decay is determined by the orientational relaxation of the nanodiscs.

The absence of dichroism under the DC electric field in TiS_2 nanodiscs studied here indicates that neither the permanent dipole nor the anisotropy of the induced dipole is sufficiently large to create an orientational order against thermal randomization. Instead, a transient orientational order created by the time-varying electric field is required to explain the observations. One possible explanation is the alignment of the nanodiscs by a transient magnetic field induced by the time-varying electric field. However, this possibility is carefully ruled out because TiS_2 nanodiscs are diamagnetic according to SQUID measurement, which can be found in Supporting Information. One may also suspect the creation of a transient magnetic field by the current generated in the nanodiscs if there are sufficient free electrons available, which may result in the transient rotational response. We ruled out this possibility, as well, because the same transient orientational order was observed not only in low-band-gap semiconducting or semimetallic TiS_2 but also in semiconducting WSe_2 and ZrS_2, with much higher band gaps, having negligible free electron density in the conduction band. When electrolytes are present in the solvent, an ionic double layer created at the interface between the material and solvent can create torques and forces in response to an electric field, such as electro-rotation and electro-osmotic effect.[24−26] In some cases, the ionic double layer introduces transient features in the electrokinetic response of the particles in aqueous solution.[23,27] However, such a possibility is also ruled out because there are no electrolytes or ionizable molecules present in the solvent medium used in this study; furthermore, the sample showed negligible charging current that would be present in the case of ionic double-layer formation (see Supporting Information). The potential influence from spatial gradients in the electric field, which may exist near the corners of the sample capillary, is also ruled out from the comparison of the electro-optic response measured in sample capillaries of different sizes (see Figure S2 in Supporting Information). In addition, the "normal" electric-field-induced dichroism of CdS nanorods observed under the identical experimental setup, as shown in Figure 1d−f, further supports that the transient electrokinetic response of TiS_2 nanodiscs is a unique material property of the colloidal TMDC nanodiscs studied here.

One possible explanation for the transient orientational order is the time-varying anisotropy of the induced dipole originating from the anisotropic dielectric relaxation under a time-varying electric field. Because of the large difference in the intralayer (covalent) and interlayer (van der Waals) bonding character, the relaxation rate of the interfacial polarization (Maxwell−Wagner−Sillars polarization) that depends on the dielectric function and conductivity of the particle and surrounding medium may be significantly distinct in different directions.[28−30] The anisotropic relaxation rate of this interfacial polarization may create a "time-varying" anisotropy of the induced dipole at the step edges of the field. If the anisotropy of the induced dipole is the largest at the field edges

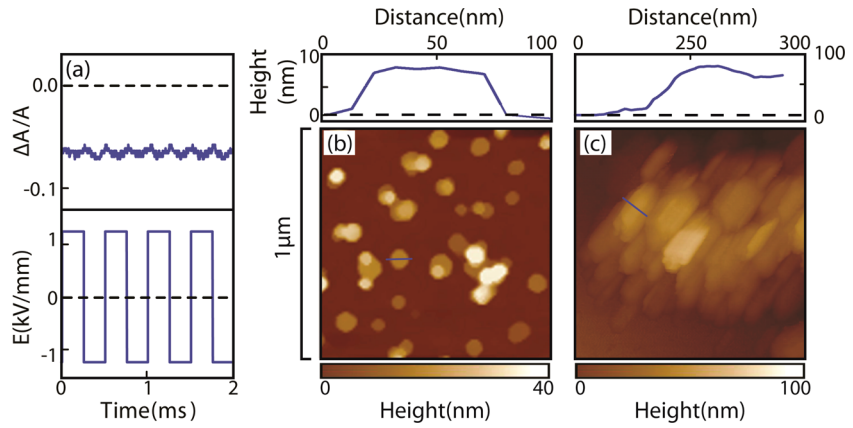

Figure 6. (a) $\Delta A/A$ under E_z square wave electric field at 2 kHz showing the near-steady-state orientational order. (b,c) AFM images of TiS_2 nanodiscs deposited on the microscope coverslip in the absence (b) and the presence (c) of the 2 kHz square wave E_z field. The average diameter and thickness of the nanodiscs are 60 and 7 nm, respectively.

and continues to decay afterward, transient orientational order can be created. However, the mechanism for the creation of the transient orientational order by the "time variation" of the electric field, not the DC amplitude of the field, is still not well-understood. Further studies will be necessary to gain a better understanding of the microscopic origin of the observed phenomena, which is beyond the scope of this study.

Nevertheless, the observed unusual transient orientational order created by the time-varying electric field in this study offers a unique insight into the new strategy for controlling the orientation of the colloidal TMDC nanoparticles that are not responsive to the DC electric field. The large disparity in the rise and decay time scales of the orientational order under the square wave field suggests that a near-steady-state orientational order may be obtained by applying an AC square wave electric field at frequencies higher than the decay rate of the orientational order. Figure 6a shows the electro-optic response ($\Delta A/A$) from TiS_2 nanodiscs under the E_z square wave field at 2 kHz, indicating that the sustaining orientational order can be obtained despite the absence of the response to DC field. To demonstrate the utility of the near-steady-state orientational order in creating the TMDC nanostructures with controlled orientation, we compared the surface orientation of TiS_2 nanodiscs on a glass substrate deposited *via* drop-casting with and without kHz square wave electric field. Figure 6b shows the atomic force microscopy (AFM) image of TiS_2 nanodiscs on a glass substrate deposited in the absence of the applied electric field. Due to the large surface area of the basal planes of TiS_2 nanodiscs interacting with the substrate, the nanodiscs prefer to lie flat on the surface as either individual or stacked discs. The line profile measured across a chosen nanodisc well represents the average diameter (~60 nm) and thickness (~7 nm) of the nanodiscs. The statistics of the measured diameter and thickness can be found in the Supporting Information. On the other hand, application of the AC square wave field at 2 kHz perpendicular to the substrate produces near-steady-state orientational order and facilitates the nanodiscs to proceed to the vertical surface orientation during the deposition, as shown in Figure 6c. The height of the structure estimated from the line profile is similar to the diameter of the nanodiscs, consistent with the vertical orientation of the nanodiscs. Meanwhile, the lateral dimensions of the nanodisc assembly are significantly larger than the height and thickness of a single nanodisc. This is due to the formation of assemblies of vertically oriented nanodiscs extended in both directions on the surface of the substrate.

To examine whether the anisotropic material properties from the orientation-controlled TiS_2 films can be obtained on a macroscopic scale, we measured the absorption spectra of TiS_2 films deposited with and without an AC square wave field over a large area. Figure 7a compares the normalized absorption spectra of the two TiS_2 film samples deposited on the microscope coverslip with (blue) and without (red) the AC square wave field measured over the area of *ca.* 5 × 5 mm^2. Figure 7b shows the photograph of the sample substrate used for the absorption measurement. In Figure 7a, the film deposited with the external electric field exhibits a significantly reduced near-infrared absorption at >700 nm compared to the film deposited without the field. This difference was reproducibly observed over multiple trials of sample preparation and measurement. The decrease in the near-infrared absorption is consistent with the reduction of the in-plane component of the optical transition in the film containing TiS_2 nanodiscs standing perpendicular to the surface compared to the case where TiS_2 nanodiscs are lying flat.[19,31] A small shift of the absorption peak in the visible spectral region in Figure 7a is also observed in the normalized comparison of the solution-phase absorption spectra for θ_p = 0 and 90° under the E_x field shown in Figure 7c. Since the solution-phase spectra for θ_p = 0 and 90° probe more in-plane and out-of-plane optical

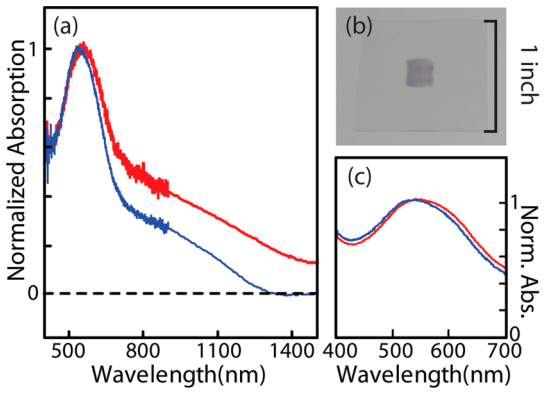

Figure 7. (a) Normalized absorption spectra of the surface-deposited samples, where TiS_2 nanodiscs were deposited on the microscope coverslip with (blue) and without (red) the applied AC square wave electric field. (b) Photograph of the microscope coverslip with the deposited TiS_2 nanodiscs. (c) Normalized comparison of the solution-phase absorption spectra for $\theta_p = 0°$ (red) and $\theta_p = 90°$ (blue) under the E_x field originally shown in Figure 4b.

transition components, respectively, than the spectrum of the randomly orientated nanodiscs, the direction of the peak shift observed in film samples is consistent with that in solution phase. Considering that other colloidal TMDC nanodiscs (WSe_2 and ZrS_2) exhibit similar transient electrokinetic response as TiS_2, the same method can be applicable to a wide range of TMDC materials that will be particularly useful in studying their anisotropic material properties, such as the anisotropic optical and interfacial charge transfer properties.

CONCLUSION

In summary, we observed the unusual electric-field-induced alignment of colloidal TMDC nanodiscs, where the orientational order was created only transiently by the time variation of the electric field, while no orientational order can be established by the DC electric field.

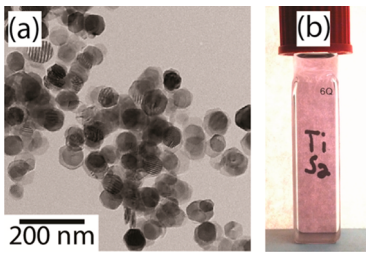

Figure 8. (a) Transmission electron microscopy image of the TiS_2 nanodiscs used in the study. (b) Photograph of the colloidal TiS_2 nanodisc solution.

The linear dichroism signal probing the orientational order under the square wave field is equivalent to performing an edge detection of the electric field, and its magnitude is dependent on the step height (ΔE) at the field edges but not on the amplitude of the field (E). This contrasts the typical response of anisotropic colloidal nanocrystals to the electric field, where the permanent dipole or (and) anisotropic-induced dipole results in a sustaining orientational order under the DC field. We conjecture that the anisotropic dielectric relaxation in the highly anisotropic TMDC nanodiscs may create a time-varying anisotropy of the induced dipole, resulting in the transient rotational order. Nevertheless, a near-steady-state orientational order could be created using an AC square wave field at frequencies higher than the orientational relaxation rate of the nanodiscs. We also showed that the near-steady-state orientational order from the AC field can be utilized to control the surface orientation of the TMDC nanodiscs deposited on a solid substrate and exhibit orientation-dependent optical properties. The ability to control the orientation of the TMDC nanodiscs demonstrated in this study will be highly valuable in exploring the anisotropic material properties of the colloidal 2D-layered TMDC nanocrystals.

METHODS

Measurement of Electro-optic Response. The colloidal TMDC nanodiscs were synthesized using the recently reported solution-phase synthesis methods.[10,32,33] The colloidal nanodisc solutions were prepared in cyclohexane at less than 0.01% volume fraction of the nanodiscs. A small amount of oleylamine (~0.5 μM) was added in solution, which facilitates the dispersion of the nanodiscs in solvent by coordinating to the edges of the nanodiscs. A transmission electron microscopy image of the TiS_2 nanodiscs and a photograph of the dilute colloidal solution are shown in Figure 8. The linear dichroism of the colloidal TMDC nanodiscs resulting from the electric-field-induced orientation was measured using a 10× microscope and a linearly polarized light source. The detailed construction of the experimental setup is shown in detail in Figure S1 of Supporting Information. Copper plates and indium-tin-oxide-coated glass plates separated by 1.3 mm were used as the electrodes, providing E_x and E_z field, respectively, as shown in Figure 2. A high-voltage amplifier (Trek 2220) or high-voltage pulse generator (DEI GRX) in combination with a function generator provided the DC or square wave voltage to the electrodes. A rectangular glass capillary with an inner dimension of 0.5 mm × 0.5 mm (VitroCom) containing the sample solution was placed between the two electrodes. Linearly polarized light in the 400−700 nm range was obtained from tungsten−halogen or a pulsed xenon lamp using a thin film polarizer. The polarization angle (θ_p) of the light is defined with respect to the direction of the E_x field. A 10× microscope objective and a tube lens were used to measure the intensity of the transmitted light from the midsection of the capillary within a 0.15 mm diameter circular area using an iris placed at the focal plane of the image. Time-dependent absorption intensity and spectrum of the sample were measured with photomultiplier tubes and a charge-coupled device spectrometer, respectively.

Preparation of Orientation-Controlled TiS_2 Nanodisc Film. Films of TiS_2 nanodiscs deposited on the microscope coverslips were prepared using the TiS_2 nanodisc solution described above. A drop of TiS_2 nanodisc solution was sandwiched between the two microscope coverslips cleaned *via* UV-ozone treatment. To confine the solution between the top and bottom coverslips and avoid drying of the solution during the deposition, a glass spacer with a 5 × 5 mm^2 square well was inserted between the two coverslips. The coverslips were placed between the two copper electrodes, providing the square wave electric field perpendicular to the surface of the substrate for 1 h.

The coverslips were removed from the electrode, separated, rinsed with chloroform, and allowed to dry. AFM (Dimension Icon) was used in tapping mode to image the surface morphology of TiS_2 nanodiscs. The film exhibiting the flat surface orientation of TiS_2 nanodiscs was prepared with the method outlined above in the absence of the electric field. The film exhibiting the vertical surface orientation of TiS_2 nanodiscs was prepared under a ~1.5 kV/mm square wave field at 2 kHz. The visible and near-infrared absorption spectra of the nanodisc films deposited on the microscope coverslip were obtained using the spectrometer equipped with Si and InGaAs detectors covering the visible and near-infrared spectral range, respectively.

Conflict of Interest: The authors declare no competing financial interest.

Supporting Information Available: The Supporting Information is available free of charge on the ACS Publications website at DOI: 10.1021/acsnano.5b01631.

Schematic of the optical microscope setup, data comparison between the thin and wide sample capillary, and data from ZrS_2 and WSe_2, SQUID measurements on TiS_2, and statistical height data from the TIS_2 nanodisc AFM images (PDF)

Acknowledgment. This work was supported by NSF (DMR-1404457) (to D.H.S.), and the Creative Research Initiative (Grant No. 2010-0018286) (to J.C.).

REFERENCES AND NOTES

1. Wang, Q. H.; Kalantar-Zadeh, K.; Kis, A.; Coleman, J. N.; Strano, M. S. Electronics and Optoelectronics of Two-Dimensional Transition Metal Dichalcogenides. *Nat. Nanotechnol.* **2012**, *7*, 699–712.
2. Chhowalla, M.; Shin, H. S.; Eda, G.; Li, L.; Loh, K. P.; Zhang, H. The Chemistry of Two-Dimensional Layered Transition Metal Dichalcogenide Nanosheets. *Nat. Chem.* **2013**, *5*, 263–375.
3. Das, S.; Chen, H. Y.; Penumatcha, A. V.; Appenzeller, J. High Performance Multilayer MoS_2 Transistors with Scandium Contacts. *Nano Lett.* **2013**, *13*, 100–105.
4. Janisch, C.; Wang, Y.; Ma, D.; Mehta, N.; Elias, A. L.; Perea-Lopez, N.; Terrones, M.; Crespi, V.; Liu, Z. Extraordinary Second Harmonic Generation in Tungsten Disulfide Monolayers. *Sci. Rep.* **2014**, *4*, 5530.
5. Splendiani, A.; Sun, L.; Zhang, Y.; Li, T.; Kim, J.; Chim, C.-Y.; Galli, G.; Wang, F. Emerging Photoluminescence in Monolayer MoS_2. *Nano Lett.* **2010**, *10*, 1271–1275.
6. Liang, W. Y. Optical Anisotropy in Layer Compounds. *J. Phys. C: Solid State Phys.* **1973**, *6*, 551–565.
7. Zeng, H.; Dai, J.; Yao, W.; Xiao, D.; Cui, X. Vally Polarization in MoS_2 Monolayers by Optical Pumping. *Nat. Nanotechnol.* **2012**, *7*, 490.
8. Cheon, J.; Gozum, J. E.; Girolami, G. S. Chemical Vapor Deposition of MoS_2 and TiS_2 Films From the Metal–Organic Precursors $Mo(S\text{-}t\text{-}Bu)_4$ and $Ti(S\text{-}t\text{-}Bu)_4$. *Chem. Mater.* **1997**, *9*, 1847–1858.
9. Zhan, Y.; Liu, Z.; Najmaei, S.; Ajayan, P. M.; Lou, J. Large-Area Vapor-Phase Growth and Characterization of MoS_2 Atomic Layers on a SiO_2 Substrate. *Small* **2012**, *8*, 966–971.
10. Han, J. H.; Lee, S.; Yoo, D.; Lee, J. H.; Cheon, J. Unveiling Chemical Reactivity and Structural Transformation of Two-Dimensional Layered Nanocrystals. *J. Am. Chem. Soc.* **2013**, *135*, 3736–3739.
11. Xia, F.; Wang, H.; Xiao, D.; Dubey, M.; Ramasubramaniam, A. Two-dimensional Material Nanophotonics. *Nat. Photonics* **2014**, *8*, 899–907.
12. Helveg, S.; Lauritsen, J. V.; Lægsgaard, E.; Stensgaard, I.; Nørskov, J. K.; Clausen, B. S.; Topsøe, H.; Besenbacher, F. Atomic-Scale Structure of Single-Layer MoS_2 Nanoclusters. *Phys. Rev. Lett.* **2000**, *84*, 951–954.
13. Rablau, C.; Vaishnava, P.; Sudakar, C.; Tackett, R.; Lawes, G.; Naik, R. Magnetic-Field-Induced Optical Anisotropy in Ferrofluids: A Time-Dependent Light-Scattering Investigation. *Phys. Rev. E* **2008**, *78*, 051502.
14. Zijlstra, P.; van Stee, M.; Verhart, N.; Gu, Z.; Orrit, M. Rotational Diffusion And Alignment of Short Gold Nanorods in an External Electric Field. *Phys. Chem. Chem. Phys.* **2012**, *14*, 4584–4588.
15. Li, L. S.; Alivisatos, A. P. Origin and Scaling of the Permanent Dipole Moment in CdSe Nanorods. *Phys. Rev. Lett.* **2003**, *90*, 097402.
16. Kundu, S.; Hill, J. P.; Richards, G. J.; Ariga, K.; Khan, A. H.; Thupakula, U.; Acharya, S. Ultranarrow PbS Nanorod-Nematic Liquid Crystal Blend for Enhanced Electro-Optic Properties. *ACS Appl. Mater. Interfaces* **2010**, *2*, 2759–2766.
17. Ryan, K. M.; Mastroianni, A.; Stancil, K. A.; Liu, H.; Alivisatos, A. P. Electric-Field-Assisted Assembly of Perpendicularly Oriented Nanorod Superlattices. *Nano Lett.* **2006**, *6*, 1479–1482.
18. Grasso, V. *Electronic Structure and Electronic Transitions in Layered Materials*; Reidel Publishing Company: Dordrecht, The Netherlands, 1986.
19. Reshak, A. H.; Auluck, S. Electronic and Optical Properties of the 1T Phases of TiS_2, $TiSe_2$ and $TiTe_2$. *Phys. Rev. B: Condens. Matter Mater. Phys.* **2003**, *68*, 245113–245120.
20. van der Zande, B. M. I.; Koper, G. J. M.; Lekkerkerker, H. N. W. Alignment of Rod-Shaped Gold Particles by Electric Fields. *J. Phys. Chem. B* **1999**, *103*, 5754–5760.
21. Kamal, J. S.; Gomes, R.; Hens, Z.; Karvar, M.; Neyts, K.; Compernolle, S.; Vanhaecke, F. Direct Determination of Absorption Anisotropy in Colloidal Quantum Rods. *Phys. Rev. B: Condens. Matter Mater. Phys.* **2012**, *85*, 035126–035132.
22. Kautek, W.; Decker, F.; Gerischer, H. Optical Anisotropy of Transition Metal Dichalcogenides. A Photoelectrochemical Determination. *Phys. Status Solidi B* **1984**, *122*, 651–659.
23. Mantegazza, F.; Caggioni, M.; Jimenez, M. L.; Bellini, T. Anomalous Field-Induced Particle Orientation in Dilute Mixtures of Charged Rod-Like and Spherical Colloids. *Nat. Phys.* **2005**, *1*, 103–106.
24. Stoyl, P. S.; Stoimenova, V. M. *Molecular and Colloidal Electro-Optics*; CRC Press: Boca Raton, FL, 2007; Vol. 134.
25. Kraemer, U.; Hoffmann, H. Electric Birefringence Measurements in Aqueous Polyelectrolyte Solutions. *Macromolecules* **1991**, *24*, 256–263.
26. Arcenegui, J. J.; García-Sánchez, P.; Morgan, H.; Ramos, A. Electro-Orientation and Electrorotation of Metal Nanowires. *Phys. Rev. E* **2013**, *88*, 063018–063029.
27. Carrasco, G. B.; Pérez Belmonte, A.; López Martinez, M. C.; García de la Torre, J. Transient Orientation and Electro-optical Properties of Axially Symmetric Macromolecules in an Electric Field of Arbitrary Strength. *J. Phys. Chem.* **1996**, *100*, 9900–9905.
28. Asami, K. Characterization of Heterogeneous Systems by Dielectric Spectroscopy. *Prog. Polym. Sci.* **2002**, *27*, 1617–1659.
29. Kohn, P.; Schröter, K.; Thurn-Albrecht, T. Interfacial Polarization and Field-Induced Orientation in Nanostructured Soft-Ion Conductors. *Phys. Rev. Lett.* **2009**, *102*, 216101–216105.
30. Saville, D. A.; Bellini, T.; Degiorgio, V.; Mantegazza, F. An Extended Maxwell–Wagner Theory for the Electric Birefringence of Charged Colloids. *J. Chem. Phys.* **2000**, *113*, 6974–6983.
31. Rossi, D.; Camacho-Forero, L. E.; Ramos-Sánchez, G.; Han, J. H.; Cheon, J.; Balbuena, P.; Son, D. H. Anisotropic Electron–Phonon Coupling in Colloidal Layered TiS_2 Nanodiscs Observed *via* Coherent Acoustic Phonons. *J. Phys. Chem. C* **2015**, *119*, 7436–7442.
32. Han, J. H.; Lee, S.; Cheon, J. Synthesis and Structural Transformations of Colloidal 2D Layered Metal Chalcogenide Nanocrystals. *Chem. Soc. Rev.* **2013**, *42*, 2581–2591.
33. Yoo, D.; Kim, M.; Jeong, S.; Han, J.; Cheon, J. Chemical Synthetic Strategy for Single-Layer Transition-Metal Chalcogenides. *J. Am. Chem. Soc.* **2014**, *136*, 14670–14673.